J Biol Inorg Chem (2014) 19:565–575
DOI 10.1007/s00775-014-1108-7

ORIGINAL PAPER

Molecular dynamics simulations of apocupredoxins: insights into the formation and stabilization of copper sites under entatic control

Luciano A. Abriata · Alejandro J. Vila · Matteo Dal Peraro

Received: 15 October 2013 / Accepted: 30 December 2013 / Published online: 30 January 2014

Abstract Cupredoxins perform copper-mediated long-range electron transfer (ET) in biological systems. Their copper-binding sites have evolved to force copper ions into ET-competent systems with decreased reorganization energy, increased reduction potential, and a distinct electronic structure compared with those of non-ET-competent copper complexes. The entatic or rack-induced state hypothesis explains these special properties in terms of the strain that the protein matrix exerts on the metal ions. This idea is supported by X-ray structures of apocupredoxins displaying "closed" arrangements of the copper ligands like those observed in the holoproteins; however, it implies completely buried copper-binding atoms, conflicting with the notion that they must be exposed for copper loading. On the other hand, a recent work based on NMR showed that the copper-binding regions of apocupredoxins are flexible in solution. We have explored five cupredoxins in their "closed" apo forms through molecular dynamics simulations. We observed that prearranged ligand conformations are not stable as the X-ray data suggest, although they do form part of the dynamic landscape of the apoproteins. This translates into variable flexibility of the copper-binding regions within a rigid fold, accompanied by fluctuations of the hydrogen bonds around the copper ligands. Major conformations with solvent-exposed copper-binding atoms could allow initial binding of the copper ions. An eventual subsequent incursion to the closed state would result in binding of the remaining ligands, trapping the closed conformation thanks to the additional binding energy and the fastening of noncovalent interactions that make up the rack.

Keywords Cupredoxins · Flexibility · Metal ion binding · Copper · Entatic state

Responsible editors: Lucia Banci and Claudio Luchinat.

This article is dedicated to the memory of Ivano Bertini, one of the founders of modern biological inorganic chemistry, friend and *maestro* of A.J.V.

L. A. Abriata (✉) · M. Dal Peraro
Laboratory of Biomolecular Modeling, School of Life Sciences, École Polytechnique Fédérale de Lausanne, Lausanne, Switzerland
e-mail: luciano.abriata@epfl.ch

L. A. Abriata · M. Dal Peraro
Swiss Institute of Bioinformatics, Lausanne, Switzerland

A. J. Vila (✉)
Instituto de Biología Molecular y Celular de Rosario (IBR, CONICET-UNR) and Área Biofísica, Facultad de Ciencias Bioquímicas y Farmacéuticas, Universidad Nacional de Rosario, Rosario, Argentina
e-mail: vila@ibr-conicet.gov.ar

Introduction

Cupredoxins are proteins with mononuclear or binuclear copper centers that perform highly efficient electron transfer through different components of the respiratory and photosynthetic chains, among others [1–4]. Efficient electron transfer requires low reorganization energies of the donor and acceptor sites so as to minimize energy losses [5, 6]; thus, the large reorganization energies associated with Cu(I)/Cu(II) couples in small complexes and protein sites not designed for electron transfer (reaching 2–2.5 eV) make them inherently poor electron transfer units. Evolution, however, has endowed cupredoxins with copper sites that display reorganization energies as low as 0.4–0.8 eV [7–9]. In these proteins, the copper site is believed to be in an energized and rigid situation, the so-

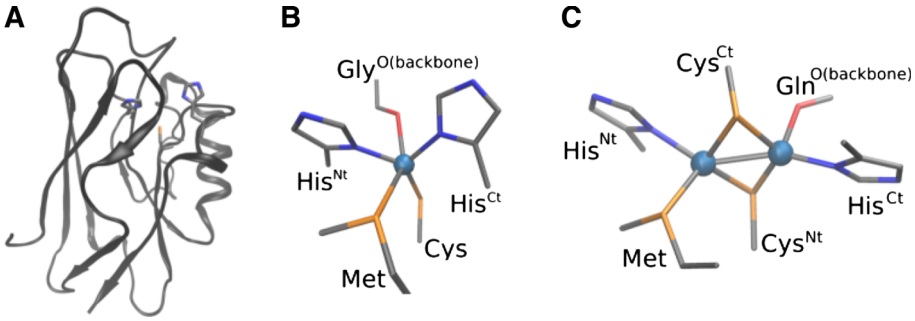

Fig. 1 **a** The cupredoxin fold as in *Pseudomonas aeruginosa* apoazurin [Protein Data Bank (PDB) ID 1E65]. **b** Mononuclear copper site from *P. aeruginosa* azurin (PDB ID 5AZU). **c** The CuA site from *Thermus thermophilus* oxidase ba_3 (PDB ID 2CUA)

called entatic or rack-induced state, that minimizes the reorganization energy of the electron transfer event and tunes the electronic properties and reduction potential of the center. The impact on these factors ultimately maximizes electron transfer rates [10].

Cupredoxins consist of a β-barrel fold with conserved histidine and cysteine residues that bind one or two copper ions together with other axial, more variable ligands (Fig. 1). In mononuclear, "type 1" cupredoxins the single copper ion is coordinated by a cysteine thiolate and the Nδ1 imidazole atoms of two histidine residues defining the core of the site, plus no, one, or two weak axial ligands that fine-tune the properties of these centers (Fig. 1b). Binuclear electron-transfer copper centers, termed "CuA sites," are also embedded in a cupredoxin fold but consist of two cysteine residues that bridge the two copper ions, whose first shells are completed with one imidazole Nδ1 atom and a weak axial ligand (Fig. 1c) [11]. The position and spacing of the copper-binding residues in the primary sequence of cupredoxins are much conserved, with one N-terminal histidine buried inside the protein and a more exposed C-terminal histidine located in a loop together with the cysteine(s) and axial ligands (Table 1) [11–17]. Outer-shell ligands are also important in defining the properties of the copper sites in cupredoxins, by assisting in the positioning of first-shell ligands and building up a rack of noncovalent interactions, most notably hydrogen bonds, around the copper site [18–21]. Owing to the structure of the protein matrix around the copper ions, the latter remain completely hidden from the solvent, just beneath the protein surface, protected from unwanted side reactions and binding of ligands. In this closed conformation, the protein matrix is believed to establish an entatic state by imposing a stiff preorganized arrangement of the copper ligands through the rack of covalent and noncovalent interactions [2, 18, 19, 22]. Early evidence to support this idea arose from X-ray structures of four copper-depleted ("apo") cupredoxins, namely, apoplastocyanin, apoazurin, apopseudoazurin, and apoamicyanin, which revealed conformations of the copper ligands nearly identical to those observed in the copper-loaded ("holo") proteins (root mean square deviation for ligands of less than 1 Å; see the example in Fig. 2a) [23–27]. However, the existence of such occluded, preformed ligand arrangements in the apoproteins is hardly compatible with the requirement of exposed copper-binding atoms to facilitate copper uptake from solution, let alone from specific chaperones as Abriata et al. [28] have shown it occurs. Indeed, in contrast with the idea of preformed ligand arrangements, recent NMR experiments on two apocupredoxins showed that the protein residues around the copper-binding regions are actually very flexible in solution at room temperature [29].

Table 1 The five proteins simulated in this work and their Protein Data Bank (*PDB*) entries

Protein	PDB ID	Copper ligands[a]
Apoplastocyanin (poplar)	2PCY	**H$_{37}$…C$_{84}$SPHQGAGM**
Apopseudoazurin (*Alcaligenes faecalis*)	1PZC	**H$_{40}$…C$_{78}$TPHYAMGM**
Apoazurin (*Pseudomonas aeruginosa*)	1E65	**H$_{46}$…C$_{112}$**TFPG**H**SAL**M**
Apoamicyanin (*Paracoccus denitrificans*)	1AAJ	**H$_{53}$…C$_{92}$TPHPFM**
Apo form of the CuA domain from *Thermus thermophilus* cytochrome *c* oxidase ba_3 (modeled by removing copper ions)	2CUA	**H$_{114}$…C$_{149}$**NQY**C**GLG**H**QN**M**

[a] Residues in *bold* are copper ligands. The numbering corresponds to the PDB entries.

To explore the flexibility of the copper-binding regions of apocupredoxins, and specifically to assess the stability of the preformed, "closed" ligand conformations observed in the X-ray structures, we performed submicrosecond molecular dynamics (MD) simulations on five protein systems. These correspond to the four mononuclear cupredoxins mentioned above, whose structures have been solved in their apo forms through X-ray crystallography, and a model of the apo form of the CuA-binding domain of subunit II of cytochrome *c* oxidase with its ligands arranged as in the holoprotein (Table 1). In all cases we found

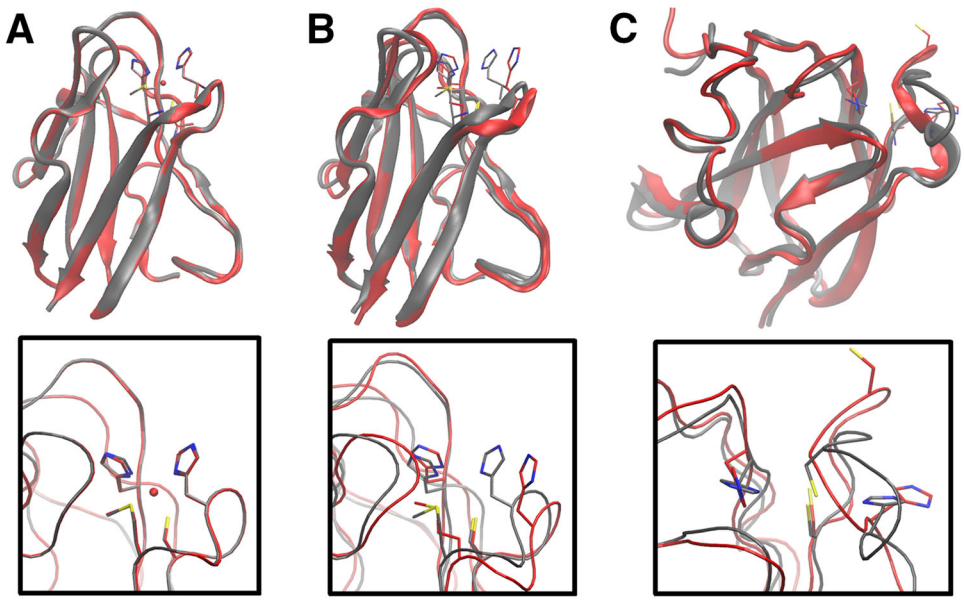

Fig. 2 **a** X-ray structures of copper-bound (*red*) and apo (*gray*) amicyanin. **b** The latter compared with a frame of the simulation with high solvent-accessible surface area (SASA) of ligands ($SASA_{ligands}$) and the C-terminal histidine flipped (*red*). **c** Starting "closed" conformation of apoCuA (*gray*) and a conformation with high-$SASA_{ligands}$ and the C-terminal histidine exposing its Nδ1 atom

that closed, prearranged conformations of the copper ligands are unstable. The copper-binding atoms all become quickly exposed during the simulations, most greatly the C-terminal histidine of the five systems and the C-terminal cysteine of the CuA-binding protein. Although the protein folds remain rigid, the copper-binding atoms exchange between exposed and closed conformations many times during the simulations. This exchange impacts on loop flexibility to a different extent in each protein, and is accompanied by continuous reshuffling of the hydrogen bonds around the copper ligands. On the basis of these observations, we propose how these metal sites might be assembled and locked into an entatic conformation.

Methods

Starting structures for MD simulations

The Protein Data Bank (PDB) structures used to set up the starting configurations are listed in Table 1. As described in "Results," four of these PDB entries correspond to the apo forms of four mononuclear cupredoxins in closed conformations very similar to those observed in the holo-proteins (azurin, pseudoazurin, plastocyanin, and amicyanin). On the other hand, the model of the apo form of a binuclear CuA protein in a closed conformation was built from the structure of the CuA-containing domain of the cytochrome *c* oxidase ba_3 from *Thermus thermophilus*. The two copper ions of its A chain were removed and the resulting thiolates were neutralized by protonation of the whole system using AmberTools . In all structures, histidine residues were protonated at their Nε2 atoms, but not at their Nδ1 atoms. This results in neutral residues consistently with a working pH of 7–8. Most importantly though, this pattern is consistent with NMR data for apoazurin, apoplastocyanin, and apoCuA [29–32] and with the hydrogen-bonding patterns deduced from the X-ray structures of these proteins [23–27, 33].

The reported NMR experiments were performed in buffers containing 20–100 mM phosphate buffer and 1–2 mM dithiothreitol, whereas the X-ray models available in the PDB arise from samples containing different kinds of cosolutes as required for crystallization of each protein. Because of this variety of conditions, the simulated systems were all set up in plain TIP3P water (plus Na^+ or Cl^- counterions to neutralize charges).

MD simulations

Simulations were run with the NAMD [34] code using the amber99SB force field [35] for the protein and TIP3P [36] parameters for water, at 300 K and 1 atm kept with a Langevin piston. The cutoff for nonbonded interactions was 12 Å, with a switching function active between 10 and 12 Å. A cutoff of 13.5 Å was used to determine the number of pairwise interactions included in the calculations of nonbonded interactions. Electrostatics were treated through particle-mesh Ewald summations with a grid spacing of 1 Å. These are all conservative parameters as shown in a

recent study by Piana et al. [37]. Each simulation box was minimized and then equilibrated by unrestrained heating in ten 30-K steps up to 300 K for a total of 1 ns, before launching the production simulations. All simulations were initially 300 ns long; the one for apoCuA was then extended to 700 ns.

Analysis of MD simulations

Trajectories were analyzed with functions and modules of the program VMD [38] together with custom MATLAB and VMD-TCL scripts. Hydrogen bonds were computed with VMD's HBond plugin. Root mean square fluctuations (RMSFs) were analyzed after alignment of the trajectories leaving out the N- and C-terminal tails so as to avoid artifacts introduced by their flexibility [39]. Equilibration periods were included in the analyses so as to see their effect on the copper-binding regions.

Results

We performed MD simulations on five systems that correspond to apocupredoxins in "closed" conformations of their copper ligands, i.e., very similar to those observed in the holoproteins (Table 1). Four of these systems correspond to actual X-ray structures of apocupredoxins, namely, apoazurin, apopseudoazurin, apoplastocyanin, and apoamicyanin [23, 25–27]. The fifth system corresponds to a model of the apo form of the CuA-binding domain of subunit II of cytochrome *c* oxidase with its ligands arranged as in the holoprotein, built by removing the copper ions from the structure of the holoprotein [33] so as to mimic a preformed chelating site analogous to that observed in the X-ray structures of the apo forms of mononuclear cupredoxins. All simulations were run in explicit TIP3P water at 300 K assuming neutral ε-protonated states for the histidine residues and neutral protonated states for the cysteines, which is consistent with a working pH of 7–8 and with the hydrogen bond patterns expected from NMR data and X-ray structures [23–27, 29–32]. Further details of the simulation setup are given in "Methods."

Simulations on the apo forms of mononuclear cupredoxins

We first describe the 300-ns-long simulations performed on the apo forms of the four mononuclear cupredoxins. As initial reaction coordinates, we monitored the extent of ligand exposure to the solvent during minimization, equilibration, and production phases in terms of the solvent-accessible surface area (SASA) of the histidine Nδ1 and cysteine Sγ atoms of the copper centers ($SASA_{ligands}$). These atoms were chosen as they are completely buried in the holoproteins but, being the main copper ligands, are expected to be at least partially exposed in conformations competent for copper capture. The possible values for $SASA_{ligands}$ range from 0 $Å^2$ (as in the starting structures, where they are all completely buried) to 97.1 and 163.06 $Å^2$ for mononuclear and CuA cupredoxins, respectively (computed from the SASA of histidine Nδ1 and cysteine Sγ atoms in the free amino acids; see caption for Fig. 3).

Figure 3 (left) shows the evolution of $SASA_{ligands}$ during the first 100 ns of the simulation for the four proteins, including the initial phase of equilibration raising the temperature from 0 to 300 K in ten steps. A logarithmic timescale was used to better show the initial evolution of $SASA_{ligands}$. The final 200 ns of the simulations are shown in Fig. 3 (right) on a linear timescale. For apoazurin, apopseudoazurin, and apoamicyanin, the initial $SASA_{ligands}$ is 0 $Å^2$ indicating that these three atoms are fully occluded in the starting structures, as in the holoproteins. However, during the equilibration period, $SASA_{ligands}$ starts to increase, indicating a large tendency of these sites to drift from the closed conformation, invariably leading to increased exposure of the copper ligands to the solvent. In the cases of apoamicyanin and apopseudoazurin, in only 2 ns $SASA_{ligands}$ is already fluctuating at around 5–10 $Å^2$, whereas for apoazurin this took 20–30 ns. These behaviors show that the ligands in the three proteins are in strained conformations that can be relaxed rapidly by exposing the copper ligands. In all cases, a large proportion of this rapid initial increase in $SASA_{ligands}$ is due to a rapid approximately 180° rotation of the imidazole group of the C-terminal histidine to expose its Nδ1 atom (Fig. 2b).

The case of apoplastocyanin is different, starting already with $SASA_{ligands}$ of approximately 7.5 $Å^2$ in the initial simulation setup. This is because the C-terminal histidine is already oriented with its Nδ1 atom exposed to the solvent in the corresponding X-ray structure. As described by the authors reporting that structure, the whole imidazole ring of the C-terminal histidine in the apoprotein seems to overlay perfectly with the same ring in the holoprotein, but the former is actually flipped, exposing its Nδ1 atom, which forms a hydrogen bond with a crystallographic water molecule [25]. If the imidazole ring of this histidine is flipped in the starting PDB structure so as to leave the Nδ1 atom in its position for copper binding, and the simulation is restarted, the imidazole ring quickly turns 180°, exposing again its Nδ1 atom (Fig. 3, left) as observed in the X-ray structure of the apoprotein and in its simulation.

The tendency and ability of the C-terminal histidine to flip exposing its copper-binding Nδ1 atom in the apoproteins suggest some degree of flexibility in this region of the

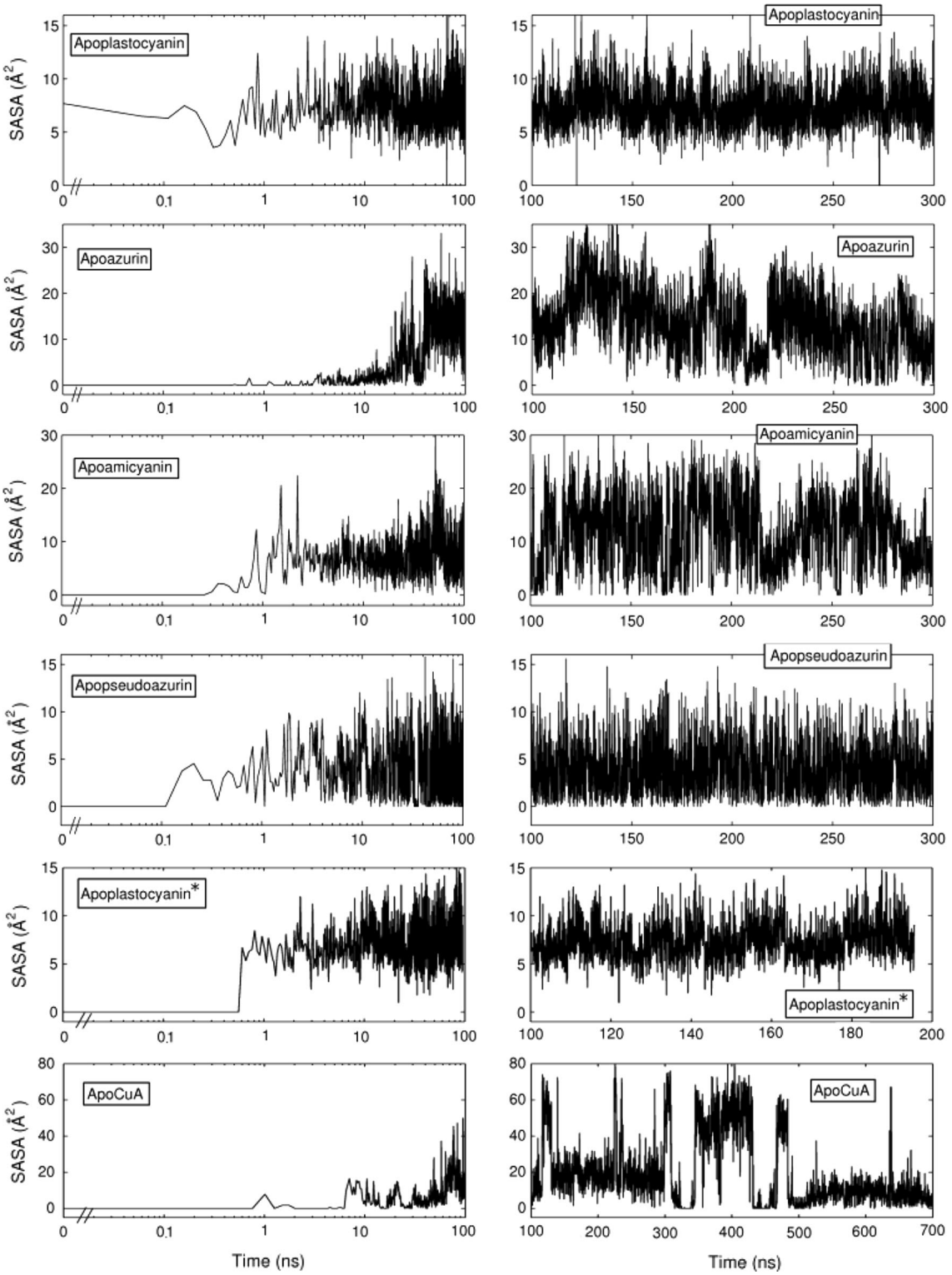

Fig. 3 SASA for histidine Nδ1 and cysteine Sγ atoms of apoplastocyanin, apoazurin, apopseudoazurin, apoamicyanin, and apoplastocyanin with its C-terminal histidine flipped as in the holoprotein (*apoplastocyanin**), and a model of the apo form of the CuA-binding domain of cytochrome *c* oxidase subunit II in a closed conformation built by removing the copper ions from the structure of the holoprotein (*apoCuA*). The *left side* shows the initial 100 ns of the simulation on a logarithmic timescale, and the *right side* shows the rest of each simulation on a linear timescale. As reference values, the maximum SASAs for the Nδ1 atom of free histidine and the Sγ atom of free cysteine are 15.57 and 65.96 Å^2, respectively (on the basis of their parameters in the AMBER99SB force field), giving maximum possible SASAs of 97.1 and 163.06 Å^2 for mononuclear and CuA cupredoxins, respectively

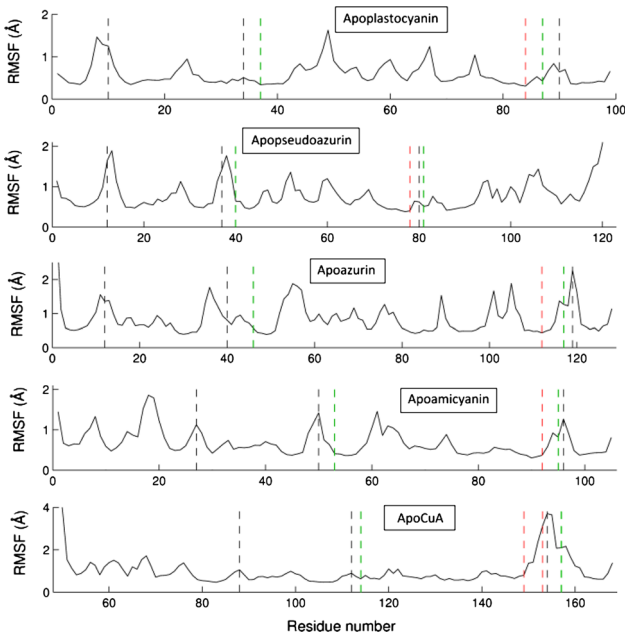

Fig. 4 Root mean square fluctuations (*RMSF*) for the Cα atoms of the five apocupredoxins simulated in this work. *Dashed green lines* and *dashed red lines* indicate the positions of copper-binding histidines and cysteines, respectively. *Dashed black lines* indicate the positions of loops around the copper sites (including those that do not contain copper ligands)

proteins. In this regard, recent NMR work reported extensive dynamics of the copper ligands in the apo forms of azurin and the CuA fragment from cytochrome *c* oxidase, which could presumably extend to all cupredoxins [29]. Following these ideas, we then analyzed the sections of the MD simulations following the initial stage in which the C-terminal histidine is exposed. Figure 3 (right) shows the time evolution of $SASA_{ligands}$ during the last 200 ns of the simulations of the four apo, mononuclear cupredoxins. In apoplastocyanin and apopseudoazurin, $SASA_{ligands}$ fluctuates around low values of approximately 5–10 $Å^2$ and approximately 2–10 $Å^2$, respectively, reaching maxima close to 15 $Å^2$ and minima of 0 $Å^2$ many times, with the C-terminal histidine remaining mostly flipped (i.e., with its Nδ1 atom exposed) and with the other ligands in a quite stable closed arrangement. In apoazurin and apoamicyanin, the $SASA_{ligands}$ fluctuations are larger, moving smoothly between values close to 0 Å, where all copper-binding atoms are hidden, to values around 25–30 $Å^2$, where not only the C-terminal histidine but also other copper ligands are exposed to the solvent. RMSF plots for Cα atoms (Fig. 4) show that the greater exposure of the copper ligands in apoazurin and apoamicyanin is paralleled by higher flexibility of the loops containing and surrounding the ligands, compared with the corresponding loops in apoplastocyanin or apopseudoazurin. In the four systems, the global folds remain largely unperturbed as shown by the low RMSF values outside loop regions.

Simulations on the apo form of the CuA fragment from *T. thermophilus* ba_3 oxidase

In the second part of this work we studied CuA sites, the other type of copper centers capable of performing efficient electron transfer, also embedded in a cupredoxin fold. With two copper ions at their core, CuA sites are optimized to perform directional electron transfer into cytochrome *c* oxidases and nitrous oxide reductases [9, 40]. A recent NMR work focusing on the apo form of the CuA-binding domain of the cytochrome *c* oxidase ba_3 from *T. thermophilus* showed that its copper-binding regions are flexible on multiple timescales in solution, resulting in an NMR-derived structure with very heterogeneous arrangements of the ligand loop, attributed to backbone dynamics [28]. MD simulations starting from this structure (PDB ID 2LLN) revealed large fluctuations of the loops that surround the copper site, but no new insights into the relationship between these flexible features and the existence, or lack, of preformed closed conformations of the copper ligands (data not shown). Certainly, this simulation might be tainted by inaccurate starting conformations of the loops that surround the copper site, owing to the very low number of NMR constraints available to properly define these flexible regions [29].

A different perspective arises from a starting structure of the apoprotein obtained by removing the two copper ions from the structure of the holoprotein (PDB ID 2CUA) to generate a model analogous to those used in the study of mononuclear cupredoxins (Fig. 2c). Figure 3 (bottom left) shows $SASA_{ligands}$ for the two histidine Nδ1 and the two cysteine Sγ atoms involved in copper binding in CuA centers. In the starting structures these four atoms are fully occluded, resulting in $SASA_{ligands}$ of 0 $Å^2$. However, during equilibration and the first few nanoseconds of the simulation, $SASA_{ligands}$ increases, revealing exposure of the copper-binding atoms as observed for the mononuclear proteins (Fig. 2c, red). This process also involves flipping of the C-terminal histidine, but more gradually than in the mononuclear proteins, being accompanied by exposure of the other ligands and slow unwinding of the ligand loop. This behavior is consistent with the idea that a stable closed conformation of the ligand loop is unlikely for apoCuA, as found for the mononuclear proteins and in agreement with the flexibility observed by NMR experiments.

As the simulation proceeds, the copper-binding atoms tend to expose more, and within a few tens of nanoseconds they have explored conformations with $SASA_{ligands}$ of approximately 10–20 $Å^2$, reaching peaks of over 40 $Å^2$ before 100 ns. We extended this simulation for a total of 700 ns, trying to capture more of these large fluctuations in

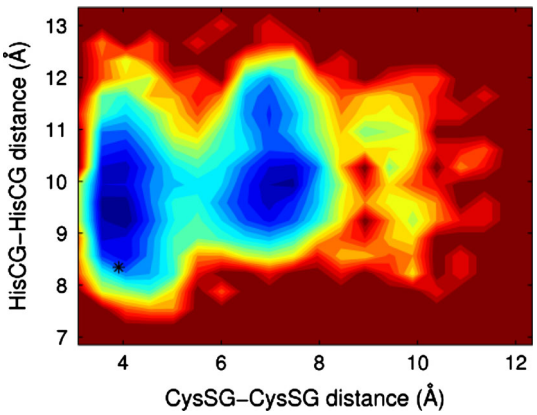

Fig. 5 Probability distribution (increasing exponentially from *blue* to *green*, to *yellow*, *orange*, and *red*, with *dark red* not being sampled) for pairs of distances between the two cysteine Sγ and the two histidine Cγ atoms of the CuA site in the simulation started from its closed conformation. The *asterisk* corresponds to the distances observed in the structure of the holoprotein

$SASA_{ligands}$. We found that the protein explores stable conformations with $SASA_{ligands}$ of 40–70 $Å^2$ many times on submicrosecond timescales (Fig. 3, bottom right). Compared with the fluctuations observed for $SASA_{ligands}$ in apoazurin and apoamicyanin, those for apoCuA are much more sudden, suggesting that the change in $SASA_{ligands}$ is linked to the exploration of two distinct conformational basins in apoCuA against simply a nearly flat surface in the mononuclear proteins. The RMSF plot for Cα atoms in apoCuA reveals high flexibility of the loop that contains the two cysteines and the C-terminal histidine (reaching an RMSF twice as large as that of the corresponding loop in apoamicyanin and apoazurin; Fig. 4) and indicates some flexibility of the two other loops that surround the CuA site, as detected by NMR, although from the experimental data, somewhat higher RMSF values could be expected.

The large RMSF peak observed in Fig. 4 for the loop containing the two cysteines and the C-terminal histidine is associated with large fluctuations of the distances between the two Nδ1 atoms and the two cysteine Sγ atoms of the site. These two distances can be regarded as reaction coordinates important to define the copper site; thus, they were explored in more detail. The probability distributions for pairs of histidine Cγ and cysteine Sγ distances are plotted as a color-coded density map in Fig. 5 (the Cγ atoms of the histidines were taken instead of the Nδ1 atom so as to remove the effects of fast flipping in the exposed one). Two main populations were found, one with a minimum close to the Sγ–Sγ and Cγ–Cγ values observed in the structure of the holoprotein (4 Å, 9.5 Å in the simulations against 4 Å, 8.5 Å from the structure as indicated by an asterisk in Fig. 5) and another that corresponds to arrangements with more separated Sγ atoms and higher $SASA_{ligands}$ (7.3 Å, 10 Å). A third, smaller population seems to be located at an Sγ–Sγ distance of 9–10 Å, but it is poorly defined in our simulation.

Discussion

Many computational studies have addressed the dynamic, structural, and electronic properties of copper-loaded cupredoxins through simulations [2, 4, 20, 21, 41–44]; however, equivalent studies on the dynamics of cupredoxins in their apo forms have been lacking. This is not a marginal omission, given that metal uptake by cupredoxins most likely occurs after synthesis of the polypeptide and folding in the adequate cellular compartment. Therefore, the structure of the apo forms is tightly related to the process of copper uptake and metal site assembly. In the five proteins here studied, we observe flexibility in at least one of the loops around the copper-binding site, resulting in an exchange of conformations with a different degree of solvent exposure of the copper-binding atoms. A recurrent feature in all our MD simulations is a preference for the C-terminal histidine's side chain to expose its Nδ1 atom, which is a copper-binding atom in the five systems. It is worth noting that the extent of flexibility predicted by the simulations is lower than that suggested by NMR spectroscopy, at least for apoazurin and apoCuA, for which NMR data are available. Although a large part of this difference is surely an unavoidable effect of limited sampling in the simulations, it is also very likely that the NMR data have overestimated the dynamics because the relevant observables (mainly a complex combination of ^{15}N chemical shift differences and relaxation rates) for residues close to truly flexible regions will be affected even if these residues are not too flexible themselves.[1]

In what follows, we discuss first the observation that predefined copper-chelating sites are unstable in the apocupredoxins, leading to exchange between exposed and buried conformations of the copper-binding atoms, and then hypothesize how such behavior could be important for the assembly of copper sites under entatic control of their properties.

Predefined arrangements of the copper ligands are unstable in apocupredoxins

All our results indicate that closed conformations of the copper ligands, in predefined positions as those observed in

[1] NMR studies pinpoint flexible residues from their nonflat R_2 relaxation dispersion profiles and from either the lack or the duplication of signals for some of their atoms. All these processes depend on the chemical shifts of the nuclei in the different exchanging populations, their interconversion rates, and their relative populations. It is hence possible that NMR data suggest mobility for nuclei which are not truly flexible but whose magnetic properties are affected by motions of nearby nuclei.

the copper-loaded proteins, are unstable in apocupredoxins. This results in variable flexibility of the loop that contains the C-terminal histidine, the cysteine(s), and the axial ligand(s), going from small fluctuations in apoplastocyanin and apoamicyanin to larger flexibility in apoazurin and apoamicyanin and very large flexibility in apoCuA. Although this variability could reflect limited sampling by the simulations and/or different timescales for motions of similar amplitudes in all the proteins, some differences across systems could be realistic since, for example, according to NMR data there are more mobile residues in the copper-binding loops of the CuA fragment than in those of apoazurin [29], and in turn many more mobile residues in these two than in apoplastocyanin [32], even when the latter is in a slightly denaturing condition.

One hallmark of all the apocupredoxins simulated here is that the C-terminal histidine is far more stable when the imidazole group is flipped by 180° relative to its position in the holoproteins, i.e., leaving its Nδ1 atom exposed to the solvent. Direct experimental support for this comes from the structure of apoplastocyanin, based on the careful analysis of electron density maps as described by Garrett et al. [25], who observed the histidine is flipped in the X-ray structure. The work of Nar et al. [23] also revealed some flexibility of apoazurin's two histidines, namely, that the copper ligands are almost superimposable with those of the holoprotein for one of the protein molecules in the unit cell but are slightly altered in the other molecule, possibly because of the presence of a water molecule in the cavity. Given that improper location of imidazole rings is not unusual in X-ray structures, and considering our results, it is plausible that the Nδ1-exposed conformation of the C-terminal histidine also holds for the other three cupredoxins. It is possible that alternative conformations of this histidine were not simple to resolve at the time of structure determination. Indeed, the electron density maps available for the structures of apoazurin, apoamicyanin, and apopseudoazurin used are not very clear about the position of the rings. In favor of the findings from our simulations, the predicted flipping to expose the Nδ1 atom is reasonable as it allows alleviation of the hindrance from at least three large electron clouds (lone pairs from both imidazole Nδ1 atoms and the large lobe from the cysteine's Sγ atom) together inside the protein cavity.

Fluctuations of the hydrogen bonds that define the rack

Outer-sphere interactions, most notably hydrogen bonds, are important elements contributing to defining and tuning the electronic structure of metal centers and have been regarded as the physical means through which the entatic state is established [10]. The first and second copper-binding shells of cupredoxins have a few conserved hydrogen bonds and other more variable hydrogen bonds straight to the ligands and around them. The conserved hydrogen bonds include the one (sometimes two) accepted by the sulfur atom of the cysteine residue in mononuclear cupredoxins or its equivalent cysteine in CuA sites (the N-terminal one), and the one donated by the Nε2 atom of the N-terminal histidine to oxygen atoms of carboxylate or amide groups buried inside the protein. All these hydrogen bonds, conserved or not among different cupredoxins, are preserved in the corresponding X-ray structures available for the four apoproteins and make part of large networks [10, 31, 45], suggesting they could be an integral part of the rack responsible for inducing the entatic state on the copper ions once bound. The conserved hydrogen bonds to the cysteine sulfur are very stable in the four mononuclear cupredoxins, with sulfur–hydrogen distances lower than 3 Å for over 80 % of the simulated time and average values of approximately 2.6 Å. In apoCuA, instead, this hydrogen bond breaks and reforms many times, existing as such for around 30 % of the simulated time. The conserved hydrogen bonds on the imidazole Nε atoms are unstable in all systems, breaking quickly and reforming only a few times.

We then looked at hydrogen bonds around the copper site more globally for our five systems by computing the total number of bonds within 5-Å spheres of the histidine and cysteine ligands (Fig. 6). The number fluctuates largely along the trajectories, staying on average around the initial number of hydrogen bonds but revealing transient states in which very few, or too many, hydrogen bonds are established compared with the initial structure. The capacity of these hydrogen bonds to reshuffle permanently while remaining stable on average despite the flexibility of the loops could be important in defining a rack around the copper sites.

Loop flexibility and metal site assembly

The observed dynamics in the copper-binding regions could be important for copper uptake by cupredoxins, either from solution or from metallochaperones, as they result in temporal exposure of the copper-binding atoms. We discuss here the implications of loop flexibility in the binding of copper ions from solution, disregarding the electrostatic effects that an approaching copper ion, either bound to a donor chaperone or free in solution, could exert on protein dynamics, as well as the effects of local ionic strengths and pH and the presence of nearby membranes or other protein complexes.

Experiments probing Cu(II) binding from solution by folded apoazurin and apostellacyanin showed that initial capture occurs through one of the histidine residues [46]. Considering such a mechanism, the stability observed for the C-terminal histidine with its Nδ1 atom exposed to the

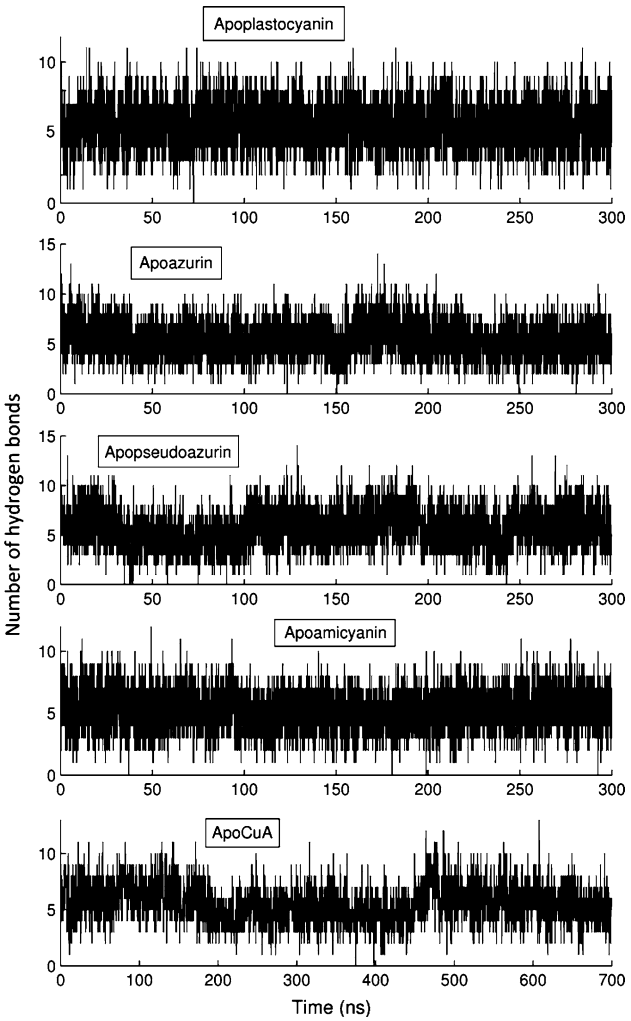

Fig. 6 Number of hydrogen bonds within a 5-Å sphere of the histidine and cysteine copper ligands along the trajectories (bonds to water molecules excluded). Data computed with the VMD using a maximum heavy atom donor–acceptor distance of 3.8 Å (instead of the default value of 3 Å, so as to pick up hydrogen bonds involving sulfur atoms) and an angle of 20° (default value in the VMD plugin)

solvent would be critical for the initial step of copper uptake into mononuclear copper sites. This is similar to an early proposition suggesting that the C-terminal histidine could act as a "revolving door" allowing the capture of copper and its assembly into the mononuclear sites [23, 25]. Our results are consistent with such an idea, in a mechanism facilitated by the flexibility of the copper-binding region. It is worth noting, however, that this flexibility is limited as shown by the RMSF profiles and the fluctuations of hydrogen bonds around the copper-binding atoms; this could allow temporal exposure of the ligands without compromising permanently the structure of the rack.

On the basis of these considerations and existing experimental data, we can depict possible mechanisms for the process of copper uptake and formation of the entatic state in cupredoxins (leaving aside changes in redox and protonation states of the cysteine and histidine residues, as MD simulations do not provide information on them and experiments are quite inconclusive). We propose that the apo forms of these proteins exist as ensembles of slightly open and closed conformations with a large preference over conformations where the C-terminal histidine's Nδ1 atom is exposed to the solvent, but eventually exploring buried conformations inaccessible to the solvent. In mononuclear cupredoxins, this histidine could initially bind copper through its exposed Nδ1 atom; then, an eventual flipping event would move the copper ion inside the protein, trapping the closed conformation through rapid binding of the other ligands (Fig. 7a). The resulting copper site would then remain locked in this rigid, occluded conformation fastened by the additional binding energy and the rack of noncovalent interactions.

A similar albeit more complex mechanism could apply to the formation of CuA centers (Fig. 7b). Experiments following binding of Cu(II) from solution [47] and Cu(I) from the periplasmic metallochaperone PCuAC show that in both cases the ions are bound sequentially, involving the existence of mononuclear intermediates [28]. According to extended X-ray absorption fine structure and absorption studies, when Cu(II) is bound from solution, an early "red-copper" intermediate is observed, presumably containing one histidine residue and two cysteine residues as in Cu(II)-loaded Sco proteins [47]. Our simulation suggests that the two cysteines become available in the open conformation of the site, i.e., that with a large Sγ–Sγ distance in Fig. 5, facilitating the formation of that red intermediate (central column in Fig. 7b). On the basis of the large flexibility of this region, it is very likely that binding of the first copper ion does not remove all the dynamic features of the ligand loop, leaving residual flexibility that allows the second ion to be accommodated. This could correspond to the fluxional mononuclear intermediate suggested by Chacón and Blackburn [47]. The histidine residue involved in initial binding of the first copper ion could be either the N-terminal histidine or the C-terminal histidine, as both are accessible in the conformation with a large Sγ–Sγ distance. We speculate that the histidine in the initial copper-capture complex is the N-terminal one, so that after the first ion is taken, the C-terminal histidine remains in a situation similar to that in the mononuclear cupredoxins, ready to take a second ion and internalize it. It is worth remarking that these conclusions and hypotheses on the formation of CuA sites are limited to the process of copper uptake from solution by a small soluble fragment of cytochrome *c* oxidase, just as in the experimental studies mentioned above. Neither our computational studies nor the reported experiments consider the effects that the rest of the oxidase and the

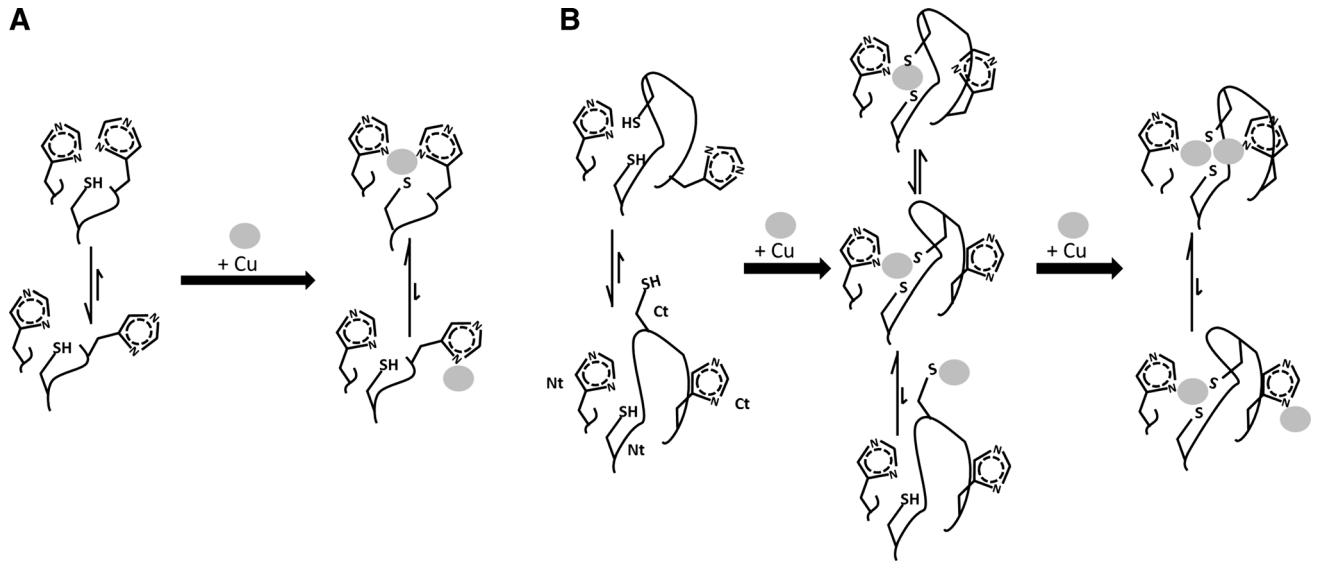

Fig. 7 Proposed roles of binding site flexibility in allowing capture of copper ions and establishment of an entatic state in mononuclear (**a**) and CuA-type (**b**) cupredoxins. *Pairs of vertical arrows* indicate exchanging conformations, their sizes reflecting qualitatively the relative populations of each state. Steps involving binding of axial ligands and changes in protonation and redox states are not considered. *Ct* C-terminal residues, *Nt* N-terminal residues

membrane might exert, which might naturally alter the dynamics of the copper-binding loops; however, given that they are quite exposed at least in bacterial oxidases, they are also likely to be somewhat flexible before metalation in vivo.

Conclusion

We have described the dynamic landscape of apocupredoxins around closed conformations of their copper-binding regions, i.e., similar to those observed in the holoproteins. Our description allows us to put together the differing outcomes from NMR and X-ray data on the apoproteins in the context of a mechanism that explains how these proteins are flexible enough to capture copper in their apo forms while forcing an entatic state on their copper ions once they are bound. We would finally like to highlight the importance of integrating X-ray structures with NMR data and MD simulations in structural studies of proteins.

Acknowledgments L.A.A. acknowledges EMBO and the Marie Curie Actions for a Long-Term Fellowship. A.J.V. is a staff member from CONICET, and work at Rosario is funded by ANPCyT (PICT-2012-1285). Dr. María Eugenia Zaballa is acknowledged for manuscript proofreading.

References

1. Gray HB, Malmström BG, Williams RJ (2000) J Biol Inorg Chem 5:551–559
2. Randall DW, Gamelin DR, LaCroix LB, Solomon EI (2000) J Biol Inorg Chem 5:16–29
3. Malmström BG (1994) Eur J Biochem 223:711–718
4. Ryde U, Olsson MH, Roos BO et al (2000) J Biol Inorg Chem 5:565–574
5. Marcus RA, Sutin N (1985) Biochim Biophys Acta 811:265–322
6. Gray HB, Winkler JR (1996) Annu Rev Biochem 65:537–561
7. Di Bilio AJ, Hill MG, Bonander N et al (1997) J Am Chem Soc 119:9921–9922
8. Farver O, Lu Y, Ang MC, Pecht I (1999) Proc Natl Acad Sci USA 96:899–902
9. Abriata LA, Álvarez-Paggi D, Ledesma GN et al (2012) Proc Natl Acad Sci USA 109:17348–17353
10. Warren JJ, Lancaster KM, Richards JH, Gray HB (2012) J Inorg Biochem 115:119–126
11. Abriata LA (2012) Acta Crystallogr Sect D 68:1223–1231
12. Sato K, Li C, Salard I et al (2009) Proc Natl Acad Sci USA 106:5616–5621
13. Velarde M, Huber R, Yanagisawa S et al (2007) Biochemistry 46:9981–9991
14. Battistuzzi G, Borsari M, Dennison C et al (2009) Biochim Biophys Acta 1794:995–1000
15. Buning C, Canters GW, Comba P et al (2000) J Am Chem Soc 122:204–211
16. Li C, Banfield MJ, Dennison C (2007) J Am Chem Soc 129:709–718
17. Yanagisawa S, Dennison C (2004) J Am Chem Soc 126:15711–15719
18. Lancaster KM, Zaballa M-E, Sproules S et al (2012) J Am Chem Soc 134:8241–8253
19. Machczynski MC, Gray HB, Richards JH (2002) J Inorg Biochem 88:375–380
20. Paltrinieri L, Borsari M, Battistuzzi G et al (2013) Biochemistry 52:7397–7404
21. Sinnecker S, Neese F (2006) J Comput Chem 27:1463–1475
22. Lancaster KM, Farver O, Wherland S et al (2011) J Am Chem Soc 133:4865–4873

23. Nar H, Messerschmidt A, Huber R et al (1992) FEBS Lett 306:119–124
24. Baker EN, Anderson BF, Blackwell KE et al (1991) J Inorg Biochem 43:162
25. Garrett TP, Clingeleffer DJ, Guss JM et al (1984) J Biol Chem 259:2822–2825
26. Petratos K, Papadovasilaki M, Dauter Z (1995) FEBS Lett 368:432–434
27. Durley R, Chen L, Lim LW et al (1993) Protein Sci 2:739–752
28. Abriata LA, Banci L, Bertini I et al (2008) Nat Chem Biol 4:599–601
29. Zaballa M-E, Abriata LA, Donaire A, Vila AJ (2012) Proc Natl Acad Sci USA 109:9254–9259
30. Hass MAS, Vlasie MD, Ubbink M, Led JJ (2009) Biochemistry 48:50–58
31. Alvarez-Paggi D, Abriata LA, Murgida DH, Vila AJ (2013) Chem Commun 49:5381–5383
32. Bai Y, Chung J, Dyson HJ, Wright PE (2001) Protein Sci 10:1056–1066
33. Williams PA, Blackburn NJ, Sanders D et al (1999) Nat Struct Biol 6:509–516
34. Phillips JC, Braun R, Wang W et al (2005) J Comput Chem 26:1781–1802
35. Hornak V, Abel R, Okur A et al (2006) Proteins 65:712–725
36. Jorgensen WL, Chandrasekhar J, Madura JD et al (1983) J Chem Phys 79:926–935
37. Piana S, Lindorff-Larsen K, Dirks RM et al (2012) PLoS One 7:e39918. doi:10.1371/journal.pone.0039918
38. Humphrey W, Dalke A, Schulten K (1996) J Mol Graphics 14:33–38
39. Caliandro R, Rossetti G, Carloni P (2012) J Chem Theory Comput 8:4775–4785
40. Abriata LA, Ledesma GN, Pierattelli R, Vila AJ (2009) J Am Chem Soc 131:1939–1946
41. Rizzuti B, Sportelli L, Guzzi R (2009) Proteins 74:961–971
42. Rizzuti B, Sportelli L, Guzzi R (2007) Biophys Chem 125:532–539
43. Gorelsky SI, Xie X, Chen Y et al (2006) J Am Chem Soc 128:16452–16453
44. Hadt RG, Sun N, Marshall NM et al (2012) J Am Chem Soc 134:16701–16716
45. Abriata LA, Vila AJ (2013) J Inorg Biochem. doi:10.1016/j.jinorgbio.2013.07.032
46. Blaszak JA, McMillin DR, Thornton AT, Tennent DL (1983) J Biol Chem 258:9886–9892
47. Chacón KN, Blackburn NJ (2012) J Am Chem Soc 134:16401–16412